Control of the Electronic Energy Transfer Pathway between Two Single Fluorophores by Dual Pulse Excitation

Burkhard Fückel,[1] Gerald Hinze,[1] Fabian Nolde,[2] Klaus Müllen,[2] and Thomas Basché[1,*]

[1]*Institut für Physikalische Chemie, Johannes Gutenberg-Universität Mainz, Jakob-Welder-Weg 11, 55128 Mainz, Germany*
[2]*Max-Planck-Insitut für Polymerforschung, Ackermannweg 10, 55128 Mainz, Germany*

We report on the control of the energy transfer pathway in individual donor-acceptor dyads by proper timing of light pulses matching the donor and acceptor transition frequencies, respectively. Excitation of both chromophores at virtually the same time induces efficient singlet-singlet annihilation, whereby excitation energy effectively flows from the acceptor to the donor. The dual pulse excitation scheme implemented here allows for all-optical switching of the fluorescence intensity at the single-molecule level. The population of higher excited states at the donor site was found to significantly increase the photobleaching probability.

PACS numbers: 33.50.−j, 31.70.Hq, 33.80.Wz, 82.37.Vb

The control of the spatial location and the internal degrees of freedom of single atoms and molecules is a central goal in nanoscience. Using low temperature scanning tunneling microscopy (STM) it has been shown that individual atoms can be arranged into a regular pattern on a substrate [1]. In the optical domain the controlled preparation of electronic [2] and spin quantum states [3] or the release of single photons on demand [4,5] are prominent examples. In the field of single-molecule spectroscopy the optical transition frequency [6] and emission intensity [7] of single molecules could be switched reversibly by light irradiation. Concerning the control of electronic coupling between individual molecules a reversible photoinduced chemical reaction was utilized to turn excitation energy transfer on and off [8]. Furthermore, entangled states of dipolar coupled molecules were created by strong light fields [9]. In a different approach energy transfer efficiencies were altered by controlling the spectral overlap through Stark-effect induced shifting of spectral lines [10]. In this Letter we report on the reversal of the energy transfer pathway in designated donor-acceptor dyads by simultaneous excitation of both chromophores.

In the case of incoherent energy transfer, which is considered here, localized excitations (Frenkel excitons) undergo a hopping type motion from donors to acceptors [11]. A straightforward approach to control the transfer efficiencies is to chemically modify the molecular structure, which in turn may result in a change of the spectral overlap between donor and acceptor and/or their separation [12–14]. Additionally, the energy flow can be manipulated by creating multiple excitations in the molecular system, which can lead to several processes. It has been observed at the ensemble [15,16] as well as at the single-molecule [17,18] level that an exciton localized at the acceptor can decrease the energy transfer rate and eventually induce emission from the donor chromophore ("exciton blockade"). On the other hand excited state annihilation processes can occur, when two or more excitations are present

at the same time [19,20]. There, energy is transferred from one electronically excited state to the other resulting in a higher excited state and a ground state. In the case of singlet-singlet annihilation (SSA) the higher excited singlet state (S_n) typically quickly relaxes to the first excited singlet state (S_1), effectively quenching one photon [19,20].

Selective excitation of the two chromophores in single donor-acceptor dyads by dual color light pulses with variable delay allowed us to create different excitation and energy transfer scenarios, which were monitored by the corresponding fluorescence signals. The investigated dyads consist of an energy donor, perylenediimide (PDI), and an acceptor, terrylenediimide (TDI), linked by two different oligo(phenylene) bridges (Fig. 1) [21]. For comparison we additionally considered single TDI molecules. The most important photophysical processes that may occur in the dyads are depicted in the inset of Fig. 1. Exciting TDI to its S_1 state leads to TDI fluorescence. On the other hand, photons absorbed by PDI are rapidly transferred to TDI, also resulting in TDI fluorescence:

$$S_1^{PDI} + S_0^{TDI} \xrightarrow{EET} S_0^{PDI} + S_1^{TDI}. \tag{1}$$
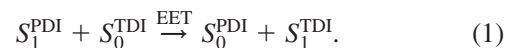
Herein, we will denote the energy transfer pathway given by Eq. (1) as EET, to discriminate it from SSA. Nevertheless, both processes are manifestations of resonant electronic excitation energy transfer. In recent studies we have quantitatively examined the EET process in the dyads **1** and **2**. It was found that the bridge effectively increases the EET rate compared to Förster's dipole-dipole model [21–23], resulting in average EET times of approximately 3 and 80 ps, for **1** and **2** at room temperature, respectively. However, if both chromophores are excited, the EET pathway is not present anymore. As mentioned above, in this case SSA as well as donor fluorescence could arise.

Single-molecule samples were prepared by standard spin coating techniques yielding thin films of PMMA
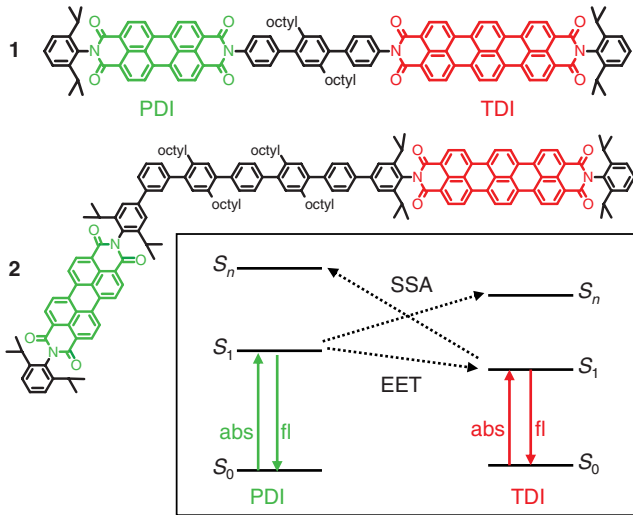
FIG. 1 (color online). Donor-acceptor dyads **1** and **2** consisting of perylenediimide (PDI) and terrylenediimide (TDI) linked by oligo(phenylene) bridges. In the inset the relevant processes upon photoexcitation are depicted. Excitation of PDI leads to electronic energy transfer to TDI (EET) and acceptor fluorescence. If both chromophores are in the first excited singlet state (S_1), in principal donor fluorescence as well as singlet-singlet annihilation (SSA) could occur.
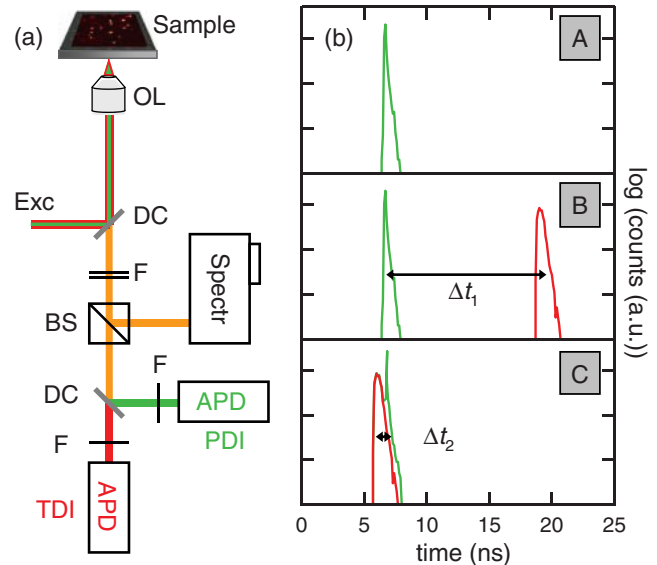

FIG. 2 (color online). (a) The confocal SMS setup. OL: objective lens, Exc: excitation light, DC: dichroic mirror, BS: 50:50 beam splitter, F: filter, Spectr: spectrograph, APD: avalanche photodiode. (b) Instrumental response functions of the three excitation sequences. During sequence A the molecules were excited by the green laser (523 or 520 nm) only. During sequence B and C we excited with red (635 nm) and green laser pulses and different time delays $\Delta t_1 = 12.5$ ns and $\Delta t_2 = -0.7$ ns, respectively.

($\sim$100 nm) doped with the dyads on a glass substrate. Dyad density was low enough to ensure spatially well separated fluorescent spots in the microscope image. During the measurements the samples were flushed with a steady argon stream to minimize oxygen induced photobleaching [24,25]. In our home-built confocal microscope [Fig. 2(a)] the excitation light was directed to the objective lens by a two-color dichroic beam splitter. The fluorescence light was collected by the same objective and split up by a 50:50 beam splitter. Half of the emission was directed to a spectrograph equipped with a CCD camera for spectral information. The other half was divided by a second dichroic mirror and detected by two APDs, such that one APD channel collected TDI emission and the other one PDI emission only. Note that the dichroic mirror in our confocal microscope did block light emitted in the region of 600–650 nm. To ensure complete spectral separation, additional filters were placed in front of the APDs. The alignment was carefully optimized by measurements with highly fluorescent polychromophoric beads until reasonable count rates were obtained on both channels.

Two pulsed laser sources were utilized: a 635 nm laser diode ("red laser") to selectively excite TDI, and a 523 nm diode-pumped Nd-YLF laser or a mode-locked Ar/Kr-ion laser operating at 520 nm ("green laser") for excitation of PDI. While the red laser was set to maximum power to saturate the $S_0 \rightarrow S_1$ transition of TDI, the green excitation intensity was considerably lower (see Table I) to prevent fast photobleaching of PDI. Note that green laser pulses have a slight chance to excite TDI, too [21]. The pulsewidths were at least 6 times smaller than the fluorescence

lifetimes of the chromophores, which are 3.8 and 3.3 ns for isolated PDI and TDI in PMMA, respectively [21].

To control the energy flow, we have employed different excitation scenarios concerning the pulse sequence. The green laser served as a trigger source pulsing with a fixed frequency of 40 MHz and constant excitation intensity throughout the experiment. The red laser pulses could be delayed electronically or selectively disabled. In this way we have implemented three different pulse sequences (A, B, C) as depicted in Fig. 2(b). In the course of period A only green pulses were used for excitation. In the second sequence (B) the red laser was enabled and both chromophores were excited with a time delay of 12.5 ns (3–4 times longer than the fluorescence decay times of the chromophores) to successively excite both chromophores. In contrast, the third sequence (C) was optimized to prepare both chromophores in the excited state at the same time. By considering the pulsewidth of the red laser and the fluorescence lifetime of TDI we calculated an optimum time delay of -0.7 ns; i.e., the red pulse arrived slightly before

TABLE I. Laser irradiance I and excitation probabilities per pulse p_{exc} at the applied laser wavelengths calculated via the absorption cross sections of the two chromophores.

λ/ nm	$I/(\mathrm{kW/cm^2})$	$p_{exc}(\mathrm{PDI})$	$p_{exc}(\mathrm{TDI})$
523	7	0.11	0.008
635	64	0	$\sim$1

the green pulse. We have applied the three pulse sequences in an alternating cycle with a repetition rate of 0.5 Hz. Note that in the cycle the duration of sequence A was 2 times the duration of B or C. In Fig. 3(a) the intensities of the reflected light of both lasers are given, which were measured separately after removal of the filters in the detection path.

Applying the excitation cycle to single TDI molecules yielded fluorescence time traces as displayed in Fig. 3(b). Trivially, the PDI channel (magnified 10 times) detected no signal. On the TDI channel, we observed nearly no fluorescence during sequence A, since the green laser pulses merely had a chance to excite TDI (c.f. Table I). As expected, during sequences B and C the fluorescence signal was almost constant. In Fig. 3(c) a section of an
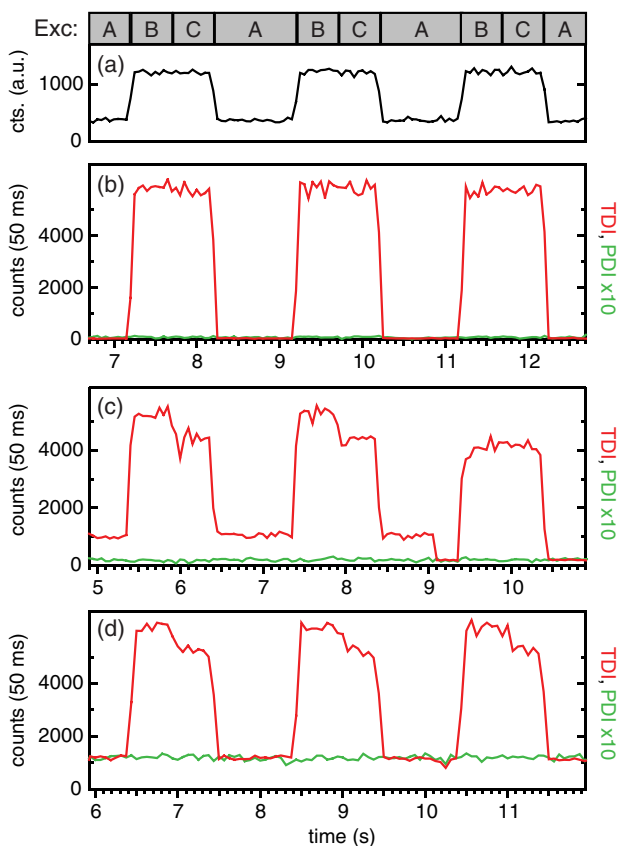

FIG. 3 (color online). (a) The excitation cycle monitored from reflected excitation light of both lasers. A, B, and C correspond to the excitation sequences displayed in Fig. 2(b). The fluorescence time traces (b)–(d) match the excitation cycle depicted in (a). (b) Fluorescence time trace of a single TDI molecule. (c) Section of an experimental time trace of dyad **1**. The emission at the TDI channel (red) showed a strong dependence on the excitation scenario. During pulse sequence C, the intensity decreased significantly compared to scenario B because of efficient SSA ($> 86\%$). The PDI channel (green, magnified 10 times) detected no fluorescence at any time. At ~ 9.1 s the donor chromophore underwent photobleaching. (d) Section of an experimental time trace of dyad **2**. A small but constant amount of PDI fluorescence (magnified 10 times) was detected in this case.

experimental time trace of dyad **1** is displayed. We found that the fluorescence intensity recorded at the TDI channel significantly changed depending on the excitation sequence. By solely exciting the donor with the green laser (sequence A), efficient EET took place. Thus, for dyad **1** only TDI emission was observed. Switching on the red laser in scenario B led to stronger TDI fluorescence. (Note that the red laser had a higher intensity than the green one.) Both the red and green excitation energies are emitted via TDI since only a single excitation was present in the molecule at a given time. In contrast, by applying sequence C both chromophores were excited at virtually the same time. Although the number of exciting photons was equal to sequence B [Fig. 3(a)], a significant decrease of the TDI fluorescence intensity was detected. On the PDI channel, during none of the three excitation sequences fluorescence was detected. Accordingly, the simultaneously recorded fluorescence spectra did not show any PDI emission. The same behavior was verified for ~ 80 dyads, which were photostable enough to be investigated for several excitation cycles.
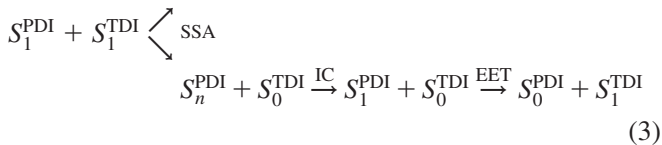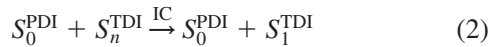
We therefore conclude that the radiative losses observed for dyad **1** stem from efficient SSA induced by pulse sequence C. For the depicted example [Fig. 3(c)] we recorded on average 1030, 5273, and 4384 counts/50 ms (less the corresponding background signal) for excitation sequences A, B, and C, respectively. Accordingly, during sequence C we recorded on average 889 counts/50 ms less than during sequence B. Assuming that the TDI chromophore was in the first excited state for every excitation induced at the PDI site by the green laser, this corresponds to a SSA efficiency of 86%. We have employed a simple rate scheme to model the SSA process, taking into account all competing processes upon excitation of both chromophores. Considering very fast internal conversion (IC) from S_n to S_1 upon singlet-singlet annihilation, for the example shown in Fig. 3(c) we obtain a SSA rate of $(0.3 \text{ ns})^{-1}$, which is 10 times faster than the competing deactivation via fluorescence emission. Since the calculation is based on the assumption that every red pulse excites TDI, the SSA efficiencies in the experiment may be actually larger than 86%. Taking into account the fact that PDI fluorescence has not been observed in the experiment, we presume an almost quantitative SSA process.

We have applied the same alternating excitation cycle on dyad **2** [Fig. 3(d)]. There, generally energy transfer processes are slower compared to **1** since the interchromophoric distance is larger [21]. This led to detectable donor fluorescence upon excitation with green light (scenario A). The weak signal of the PDI channel, however, remained approximately constant for all excitation sequences, implying that the SSA dynamics in dyad **2** is on the same time scale as the EET process. The aforementioned analysis of the fluorescence signal registered in the TDI channel resulted in a lower limit for the SSA efficiency of 79% for the depicted example, corresponding to a SSA rate of $(0.5 \text{ ns})^{-1}$.

TABLE II. Relative photobleaching probabilities for the PDI chromophore in dyads **1** and **2** in dependence of the pulse sequences. Please note that these relative probabilities have been calculated for unit time. The total numbers of molecules where PDI bleached first were: 52 (**1**) and 75 (**2**).

Dyad	Relative bleaching probabilities		
	A	*B*	*C*
1	14%	22%	64%
2	16%	22%	62%

In principle, in the dyads the SSA process may occur in two directions:

$$S_0^{PDI} + S_n^{TDI} \xrightarrow{IC} S_0^{PDI} + S_1^{TDI} \tag{2}$$

$$S_1^{PDI} + S_1^{TDI} \nwarrow_{SSA}$$

$$S_n^{PDI} + S_0^{TDI} \xrightarrow{IC} S_1^{PDI} + S_0^{TDI} \xrightarrow{EET} S_0^{PDI} + S_1^{TDI} \tag{3}$$

In both cases TDI fluorescence is recorded, making a simple spectral distinction impossible. However, we have compared the spectral overlaps for the two SSA processes possible. The PDI $S_1 \to S_n$ excited state absorption has been investigated experimentally and theoretically [26], while the TDI $S_1 \to S_n$ excited state absorption has been measured by transient absorption spectroscopy. Compared to EET, the spectral overlap (of SSA) has a 5 times smaller and a 2 times larger value for pathways (2) and (3), respectively. From that we conclude that the energy is preferentially transferred to PDI, thus promoting it to a higher singlet state as depicted in pathway (3).

Concerning the photostability [24,25], we observe that in both dyads the PDI chromophore is significantly less photostable than TDI [21]. Interestingly, with the experiment presented herein, we may easily detect which chromophores of the investigated dyads are intact at a given instant of time. Photobleaching of PDI resulted in almost no fluorescence signal during excitation sequence *A*, while *B* and *C* led to constant TDI fluorescence. An example is displayed in Fig. 3(c). Here, at ~9.1 s the PDI chromophore underwent photobleaching and consequently an emission pattern similar to that of single TDI molecules [c.f. Fig. 3(b)] was observed.

Throughout the *A-B-C* cycle the excitation of PDI by the green laser remained constant. Assuming the photobleaching of PDI to be independent of the pulse sequence, a ratio corresponding to the duration, i.e., 2:1:1 for *A:B:C*, respectively, is expected. Remarkably, we found that in more than half of all cases the irreversible photobleaching of PDI originated from excitation scenario *C* (see Table II), almost a threefold higher probability compared to *B*. This finding not only corroborates that SSA occurs preferentially at the donor site during sequence *C* [pathway (3)] but also nicely confirms the common assumption that higher excited states are prone to photobleaching [24].

Summarizing, by applying pulse sequence *C* the energy transfer pathway in the dyads has been reversed. Each green excitation that is created at the PDI site will promote the PDI to a higher excited state by annihilating a red excitation from the TDI site. By this means energy effectively flows from the former acceptor to the former donor. Since the time delay between green and red pulses allows for controlling the TDI fluorescence signal level, besides reversal of energy transfer a novel scheme for all-optical switching at the single-molecule level has been implemented. Note that by increasing the excitation rate for PDI, the amount of radiative losses can be enhanced for a given pulse sequence. Further work will monitor the system response for a number of time delays and excitation intensities. Finally, through preparation of higher excited states via SSA, a new window for the study of single-molecule photobleaching processes has been opened.

*Corresponding author.
Thomas.Basche@uni-mainz.de

[1] D. M. Eigler and E. K. Schweizer, Nature (London) **344**, 524 (1990).
[2] W. Nagourney, J. Sandberg, and H. Dehmelt, Phys. Rev. Lett. **56**, 2797 (1986).
[3] F. Jelezko *et al.*, Phys. Rev. Lett. **92**, 076401 (2004).
[4] B. Lounis and W. E. Moerner, Nature (London) **407**, 491 (2000).
[5] P. Michler *et al.*, Science **290**, 2282 (2000).
[6] F. Kulzer *et al.*, Nature (London) **387**, 688 (1997).
[7] M. Heilemann *et al.*, J. Am. Chem. Soc. **127**, 3801 (2005).
[8] M. Irie *et al.*, Nature (London) **420**, 759 (2002).
[9] C. Hettich *et al.*, Science **298**, 385 (2002).
[10] K. Becker *et al.*, Nature Mater. **5**, 777 (2006).
[11] T. Förster, Ann. Phys. (Leipzig) **437**, 55 (1948).
[12] R. P. Haugland, J. Yguerabide, and L. Stryer, Proc. Natl. Acad. Sci. U.S.A. **63**, 23 (1969).
[13] R. K. Lammi *et al.*, J. Am. Chem. Soc. **122**, 7579 (2000).
[14] T. Q. Nguyen *et al.*, Science **288**, 652 (2000).
[15] R. Augulis *et al.*, J. Phys. Chem. A **111**, 12 944 (2007).
[16] F. V. R. Neuwahl *et al.*, J. Phys. Chem. B **105**, 1307 (2001).
[17] A. J. Berglund, A. C. Doherty, and H. Mabuchi, Phys. Rev. Lett. **89**, 068101 (2002).
[18] M. J. Walter *et al.*, Nano Lett. **8**, 3330 (2008).
[19] J. Hofkens *et al.*, Proc. Natl. Acad. Sci. U.S.A. **100**, 13 146 (2003).
[20] C. G. Hübner *et al.*, Phys. Rev. Lett. **91**, 093903 (2003).
[21] G. Hinze *et al.*, J. Chem. Phys. **128**, 124516 (2008).
[22] B. Fückel *et al.*, J. Chem. Phys. **128**, 074505 (2008).
[23] R. Métivier *et al.*, Phys. Rev. Lett. **98**, 047802 (2007).
[24] R. Zondervan *et al.*, J. Phys. Chem. A **108**, 1657 (2004).
[25] T. Christ *et al.*, Angew. Chem., Int. Ed. **40**, 4192 (2001).
[26] E. Engel *et al.*, Phys. Rev. B **73**, 245216 (2006).